Clin Neuroradiol (2015) (Suppl) 25:219–224
DOI 10.1007/s00062-015-0433-8

REVIEW ARTICLE

Quantitative MR Imaging of Brain Tissue and Brain Pathologies

E. Hattingen · A. Jurcoane · M. Nelles · A. Müller · U. Nöth · B. Mädler · P. Mürtz · R. Deichmann · H. H. Schild

Received: 3 April 2015 / Accepted: 1 July 2015 / Published online: 30 July 2015

Abstract Measurement of basic quantitative magnetic resonance (MR) parameters (e.g., relaxation times T1, T2*, T2 or respective rates R (1/T)) corrected for radiofrequency (RF) coil bias yields different conventional and new tissue contrasts as well as volumes for tissue segmentation. This approach also provides quantitative measures of microstructural and functional tissue changes. We herein demonstrate some prospects of quantitative MR imaging in neurological diagnostics and science.

Keywords qMRI · T2-relaxation time · T1-relaxation time · BOLD · TOLD

E. Hattingen (✉) · A. Jurcoane · M. Nelles · A. Müller · P. Mürtz
Neuroradiologie, Radiologische Klinik des Universitätsklinikums Bonn,
Sigmund Freud Strasse 25,
53127 Bonn, Germany
e-mail: elke.hattingen@ukb.uni-bonn.de

U. Nöth · R. Deichmann
Brain Imaging Center, Universitätsklinikum Frankfurt,
Frankfurt/Main, Germany

B. Mädler
Philips Medical Systems, Philips GmbH,
Hamburg, Germany

H. H. Schild
Radiologische Klinik des Universitätsklinikums Bonn,
Sigmund Freud Strasse 25,
53127 Bonn, Germany

Introduction

Interpretation of conventional diagnostic magnetic resonance (MR) images is often hampered by the fact that data acquired at different sites are not necessarily comparable. This may be due to

1. Differences in the magnetic field strength
2. Different hardware characteristics of the scanners, like magnetic field inhomogeneities (B0), and the RF coils used with their respective transmit and receive profiles (B1)
3. Variations in software for programming MR sequences or the choice of imaging parameters (e.g., repetition time (TR), echo time (TE), slice thickness, and orientation).

Furthermore, diffuse brain pathologies or subtle signal changes may not be visible on conventional MR imaging (MRI) scans. Therefore, a precise morphological picture of the pathology (focal or diffuse) as well as an objective, reliable, and sensitive characterization of MR-accessible tissue parameters is needed. While conventional MRI is optimized to show morphology by using several sequences with different contrasts, quantitative (q)MRI methods may support tissue characterization by mapping of certain MR tissue parameters such relaxation times T1, T2*, T2 or the respective rates (R=1/T) but also proton density (PD), etc. Most qMR approaches comprise measurement series that vary one parameter (e.g., flip angle, inversion time, or echo time), and the thereof calculated qMR value is a function of the resulting signal intensity changes. Inhomogeneities of B0 or B1 are averaged out by the measurement series or they are directly measured and corrected thereafter [1]. Compared to conventional MR, qMR parameter maps are more reliable since they are ideally independent from scanner hardware and software (see points 2 and 3 above)

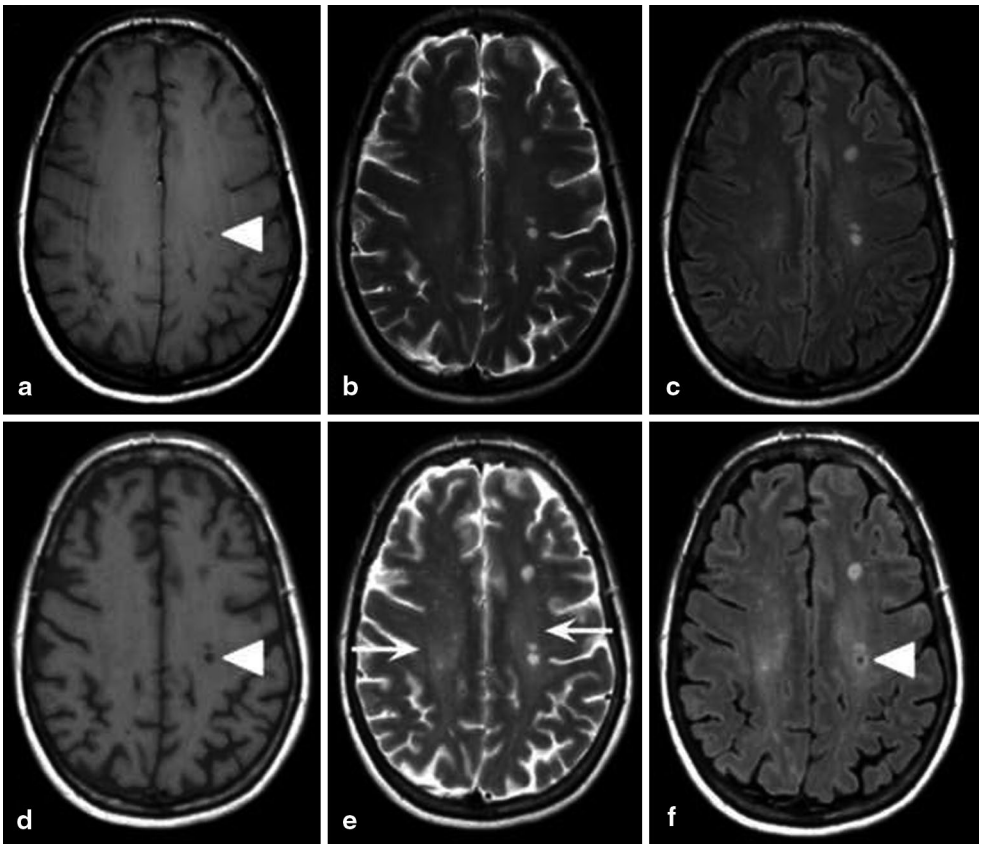

Fig. 1 Synthetic MRI for standard sequences of a patient with multiple sclerosis (MS). The *upper* row shows a conventional **a** T1-weighted image with TR = 624 ms and TE = 13 ms, **b** T2-weighted image with TR = 3277 ms and TE = 80 ms, and **c** Fluid-attenuated inversion recovery (FLAIR) with TR = 12000 ms, TE = 140 ms, and inversion time (TI) = 2850 ms. The *lower* row shows the respective synthetic images with simulated **d** TR = 500 ms, TE = 10 ms; **e** TR = 4000 ms, TE = 100 ms; and **f** TR = 12000 ms, TE = 100 ms, and TI = 2600 ms. Diffuse white matter damage in MS ("Dirty" white matter) is better demonstrated in the synthetic T2-weighted image (*arrows* in **e**). The synthetic FLAIR image (**f**) reveals more T1 contrast showing the *black hole* visible in the T1-weighted images (*arrowhead* in **a, d, f**)

and thus the acquisition site. In addition, the acquisition of basic MR parameter maps also allows for the calculation of synthetic MR images (examples 1 and 2) with optimized tissue contrasts for depicting various anatomical structures and brain pathologies. High-resolution relaxation time maps (example 3) also allow for segmentation of gray and white matter by exploiting their different ranges of T1 relaxation time. In addition, pathophysiological changes in deoxygenated hemoglobin (dHb) or tissue oxygenation are quantifiable with qMR methods (example 4).

For the detailed description of qMR methods, we refer to the respective reviews [1, 2].

The first studies evaluating the benefits of cerebral qMRI aimed to identify pathologies based on relaxation times and proton density changes. However, with relaxation times of different pathologies overlapping considerably [3–5], more complex tissue characterization came into focus, for example, those based on water diffusion, magnetization transfer, and perfusion. It became obvious that the strengths of quantitative or semi-quantitative MR parameter maps lie in the detection of diffuse changes in brain tissues that appeared normal in conventional MRI [6–8], best demonstrated in multiple sclerosis patients [2, 7, 9–14].

Current advances in MR imaging techniques, hardware development, and post-processing methods pave the way to a new generation of qMRI applications. Once quantitative maps of T1, T2, T2*, PD, magnetic field inhomogeneities B0, and RF coil inhomogeneities (B1 and receive profile) are determined, these data can be used for a wide range of applications. In the following, we will give a pictorial overview of the different capabilities of qMRI. For more details on data acquisition and post processing, the reader is referred to the references in the respective examples.

Example 1: Synthetic MRI for Standard Sequences

Quantitative parameter maps of T1- and T2-relaxation times and B1 provide information to generate synthetic MR images with any combination of calculated parameters and removed B1 influences. The weights of the T1- and T2-values may vary with the TR and TE, which have to be chosen before conventional MR data acquisition. In contrast, quantitative data and the respective post-processing software allow simulating different TR and TE to generate multiple weights afterwards.

Figure 1 shows conventional "weighted" images (a–c) and the respective synthetic images (d–f) of a patient with multiple sclerosis. The qMR measurement and processing of the respective synthetic images (d–f) based on the QRAPMASTER method [15]. Since we calculated synthetic images to optimize the diagnostic value, the TR and

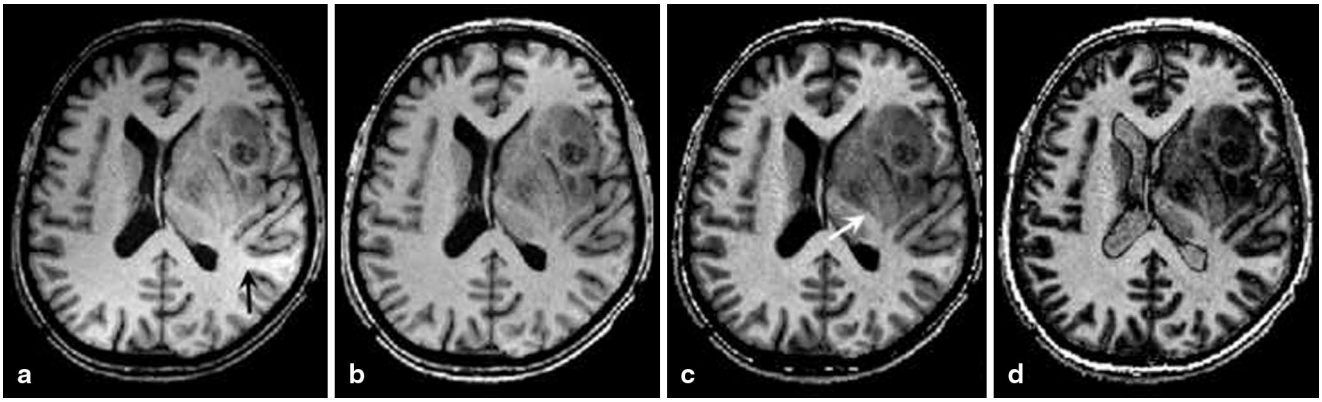

Fig. 2 Synthetic MRI to create new contrasts. Three synthetic MP-RAGE images based on a 1 mm-isovolumetric FLASH-EPI hybrid readout consisting in a PD-weighted and T1-weighted dataset via different excitation angles. MP-RAGE images were calculated by imitating **a** standard acquired MP-RAGE image with T1 weighting and additional influence from PD (T1-PD-weighting); **b** MP-RAGE image with T1-PD-weighting but without RF coil bias, eliminating false hyperintense signal in the left parietal brain (*black arrow* in a); **c** MP-RAGE image with T1-weighting only and without RF coil bias; and **d** synthetic IR image with pure T1-weighting. The purely T1-weighted MP-RAGE image (**c**) provides the best contrast for tumor delineation and clearly reveals infiltration of basal ganglia (*white arrow*). The purely T1-weighted synthetic IR image (**d**) also provides excellent delineation of tumor and tumor margins (TI = 1300 ms)

TE differed from the institutional standard parameters of conventional MR images.

The conventional sequences take about 2 min each (FLAIR 2:00 min; T1-w sequence 2:09 min; T2-w sequence 1:58 min), summing up to a total scan time of 6:07 versus 4:52 min for the acquisition of the quantitative sequence. However, qMRI is still not ready to replace conventional MRI, since longer measurement times are needed to generate high-quality synthetic images with a high spatial resolution (see example 2).

Example 2: Synthetic MRI to Create New Contrasts

Apart from imitating contrasts of conventional MRI, qMR data allow generating new contrasts to optimize the delineation of brain pathologies. Brain tumor tissue, for example, has elevated T1 and PD values; which inversely influence the signal in T1-weighted images, resulting in partial masking of the tumor. QMR techniques allow for the creation of purely T1-weighted synthetic images, thus improving tumor-to-background contrasts [16].

Figure 2 shows a patient with a glioblastoma in the left hemisphere infiltrating the basal ganglia. From these qMR data, three synthetic magnetization-prepared rapid gradient-echo (MP-RAGE) images were calculated (a–c) by replicating standard acquired MP-RAGE images (a). The synthetic MP-RAGE image with T1-PD-weighting, but without RF coil bias (b) is free of the false hyperintense signal from B1 inhomogeneities. The purely T1-weighted MP-RAGE image (c) provides the best contrast for tumor delineation and clearly reveals infiltration even of gray matter. The synthetic inversion recovery (IR) image (d) with pure T1-weighting also provides excellent delineation of tumor and tumor margins. The qMR sequence was based on the variable flip angle technique using a FLASH-EPI hybrid readout [16, 17] with a duration of 9:48 min. In addition, B1 mapping was performed according to the method described by Volz et al. [18].

Example 3: Quantitative Maps to Measure Tissue Changes

Quantitative mapping of relaxation times T1 and T2 as basis of qMR provides objective measurement of brain tissue alterations and the T1 shortening after application of a contrast agent. T1 shortening indicates interstitial accumulation of the contrast agent and hence blood–brain barrier breakdown in the brain.

T1 Mapping (Fig. 3a)

Longitudinal (spin-lattice) relaxation time T1 can be measured by the IR method described by Freemann et al. [19]: After a 180° RF pulse, the longitudinal magnetization recovers its equilibrium value with the time constant T1. Nowadays, the use of 1 mm-isovolumetric 3D sequences allows segmenting gray and white matter as well as detecting even subtle brain tissue alterations. Figure 3a demonstrates the method: A series of five 3D IR-TFE sequences with IR = 150, 350, 750, 1200, and 2300 ms was acquired once before (pre) and once after intravenous application of a contrast agent (post). Each of the five IR-TFE sequences lasted 1:33 min. Images acquired at increasing times after the RF pulse reveal the signal recovery, while the quantita-

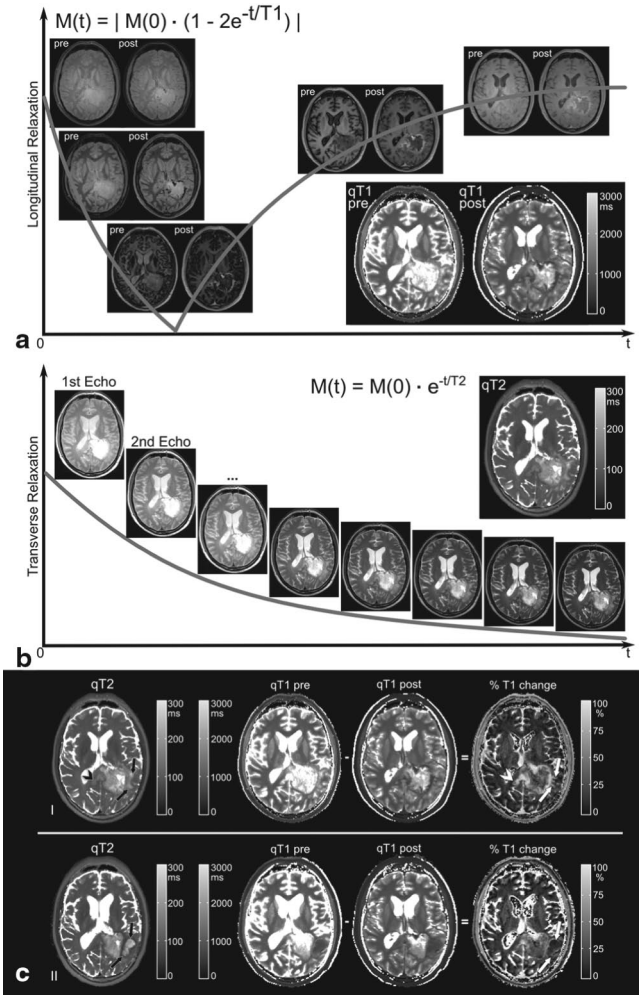

Fig. 3 Quantitative maps to measure tissue changes. Mapping of T1 relaxation time using the IR method (**a**) and mapping of T2 relaxation time (**b**) are shown in a patient with glioblastoma 18 days after surgery (**c**I) and 42 days after starting radiation with concomitant temozolomide (**c**II). Although single images in (**a**) and (**b**) are "weighted," most of these images do not have "reasonable" contrast to look at. Instead, these measurements are translated into quantitative maps (**c**) giving gray-coded relaxation times in [ms] for each voxel. Quantitative maps (cI) show reactive changes and residual tumor (increased T2 and T1-shortening measured in %T1 change map) in the splenium of the corpus callosum (*arrowhead*). In the surrounding "edema" (*black arrows*), striated enhancement also reveals tumor infiltration (*white arrows*). During combined radiochemotherapy (cII), reactive changes as well as the tumor-associated lesion in the splenium of the corpus callosum (qT2 and %T1) regressed. A new hematoma (*arrows* in cI) with increased T2 (*black arrows*) and short T1 (*white arrows*) occurred in the infiltration zone

tive T1 (qT1) map depicts the tissue-specific longitudinal relaxation time (in ms) in each voxel. After (post) contrast agent administration, the magnetization recovers faster (due to a lower T1) than before (pre). This effect is most pronounced in regions with higher enhancement due to blood–brain barrier breakdown around the resection cavity.

T2 Mapping (Fig. 3b)

The measurement of transverse (spin–spin) relaxation time T2 is shown in Fig. 3b: After a 90° RF pulse, the transverse magnetization decays with the time constant T2. Images acquired with increasing echo times TE of 15, 30, 45, 60, 75, 90, 105, and 120 ms reveal the signal decay, while the quantitative T2 (qT2) map depicts the tissue-specific transverse relaxation time (in ms) in each voxel. Scan duration was 9:33 min.

Quantitative Maps in a Patient with a Brain Tumor (Fig. 3c)

Quantitative T1 and T2 maps sensitively monitor the reaction of brain tumors during treatment [20, 21]. Figure 3c shows an example of a patient with glioblastoma. In areas with increased T2, %T1 change maps [14] may detect even subtle tumor infiltration by quantifying the degree of T1 shortening after interstitial accumulation of the contrast agent.

Example 4: R1 and R2* Changes During Respiratory Challenges to Assess Tumor Oxygenation and Vascular Reactivity

A dynamic T1-weighted short TR steady-state spoiled multi-gradient-echo sequence (dSSPMGE) enables to map simultaneously changes in the relaxation rates R2* and R1 (dR2*, dR1) of normal and tumor tissue during inhalation of carbogen (Cb5) and 5 % carbon dioxide in air (CO_2-air) [22]. The sequence dynamically measures dR2* and dR1 over a period of 7:52 min. Prior to this sequence, R1 baseline measurement (2:38 min) and B1 mapping (0:46 min) are performed. The inhalation of carbogen or CO_2 in air leads to changes in the amount of dHb and oxygen molecules dissolved in plasma and tissue. The dHb and molecular oxygen are both paramagnetic and hereby influence R2* and R1. The longitudinal relaxation rate R1 linearly increases with the concentration of molecular oxygen. This approach provides the basis for the so-called tissue-oxygen-level-dependent (TOLD) imaging [23]. The R2* approach is called blood-oxygen-level-dependent (BOLD) imaging, because the relaxation rate R2* is directly related to the dHb concentration in blood vessels [24].

Figure 4 displays T2- and T1-weighted images after contrast administration of a patient with a partially hemorrhagic glioblastoma (a). The dR2* and dR1 maps (b) assess the oxygenation and vasoreactivity of the tumor tissue during carbogen inhalation [22]. The tumor area (white arrow) shows a strong R2* and R1 decrease during carbogen inhalation consistent with low baseline oxygenation, mainly

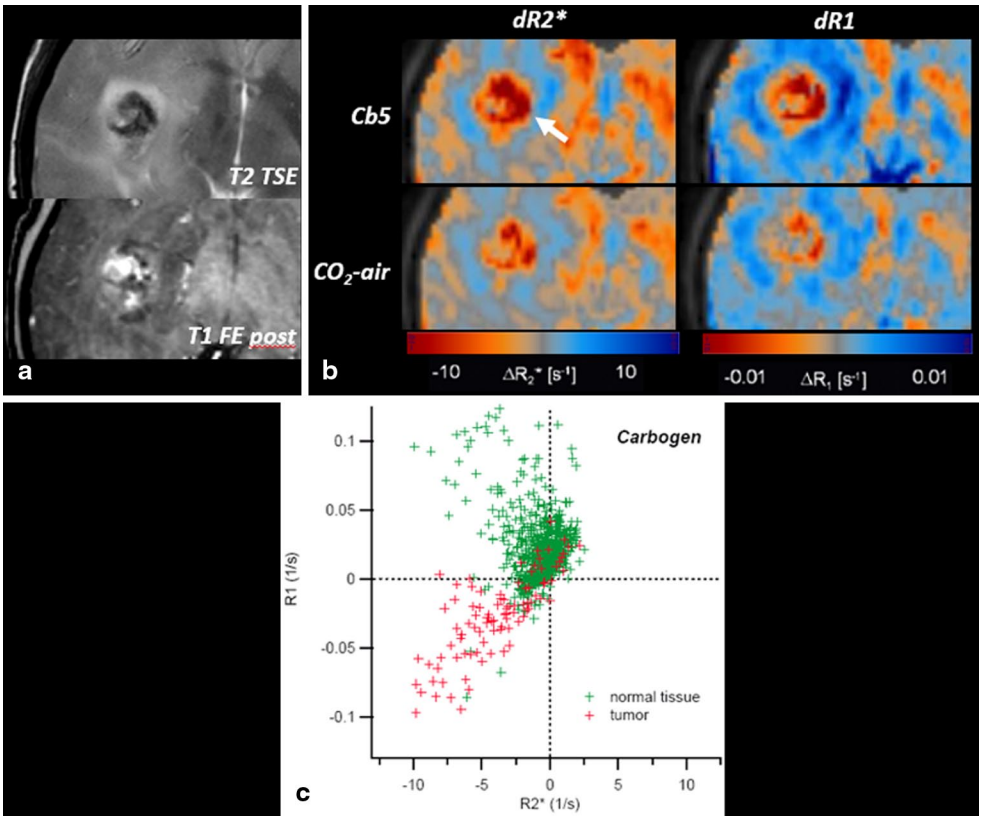

Fig. 4 R1 and R2* changes during respiratory challenges to assess tumor oxygenation and vascular reactivity. In contrast to Figs. 1–3, a dynamic quantitative sequence (dSSPMGE) simultaneously measured changes in relaxation rates R2* and R1 over time. This research measurement was performed to assess glioblastoma oxygenation and vascular reactivity. Detailed description is given in the respective section of example 4

driven by erythrocyte perfusion. The R2* decrease at inhalation of 5% CO_2 in air indicates preserved vasoreactivity from relatively mature tumor vessels equipped with smooth musculature. The scatter plot of dR2* and dR1 (c) illustrates the different response patterns of tumor (red crosses) and normal tissue (green crosses) during carbogen breathing. In fig 4c, normal tissue (contralateral gray and white matter) mainly clusters in the left upper quarter ($dR2^* < 0$ and $dR1 > 0$), consistent with a normal oxygenation status. Tumor tissue shows strong negative values (dR2* and $dR1 < 0$), pointing to a dominant BOLD effect because of low baseline oxygenation [25].

Conflict of Interest B. Mädler is an employee of Philips Medical Systems, but he has no conflict of interest in this review. The authors declare that they have no conflict of interest.

References

1. Cheng HL, Stikov N, Ghugre NR, Wright GA. Practical medical applications of quantitative MR relaxometry. J Magn Reson Imaging. 2012;36:805–24.
2. Tofts P, editor. Quantitative MRI of the brain: measuring changes caused by disease. Chichester: Wiley; 2003. pp. 272–98).
3. Komiyama M, Yagura H, Baba M, Yasui T, Hakuba A, Nishimura S, Inoue Y. MR imaging: possibility of tissue characterization of brain tumors using T1 and T2 values. AJNR Am J Neuroradiol. 1987;8:65–70.
4. Kjaer L, Thomsen C, Gjerris F, Mosdal B, Henriksen O. Tissue characterization of intracranial tumors by MR imaging. In vivo evaluation of T1- and T2-relaxation behavior at 1.5 T. Acta Radiol. 1991;32:498–504.
5. Hoehn-Berlage M, Bockhorst K. Quantitative magnetic resonance imaging of rat brain tumors: in vivo NMR relaxometry for the discrimination of normal and pathological tissues. Technol Health Care. 1994;2:247–54.
6. Miot E, Hoffschir D, Alapetite C, Gaboriaud G, Pontvert D, Fetissof F, Pape AL, Akoka S. Experimental MR study of cerebral radiation injury: quantitative T2 changes over time and histopathologic correlation. AJNR Am J Neuroradiol. 1995;16:79–85.
7. Parry A, Clare S, Jenkinson M, Smith S, Palace J, Matthews PM. White matter and lesion T1 relaxation times increase in parallel and correlate with disability in multiple sclerosis. J Neurol. 2002;249:1279–86.
8. Mamere AE, Saraiva LA, Matos AL, Carneiro AA, Santos AC. Evaluation of delayed neuronal and axonal damage secondary to moderate and severe traumatic brain injury using quantitative MR imaging techniques. AJNR Am J Neuroradiol. 2009;30:947–52.
9. Vrenken H, Geurts JJ, Knol DL, Polman CH, Castelijns JA, Pouwels PJ, Barkhof F. Normal-appearing white matter changes vary with distance to lesions in multiple sclerosis. AJNR Am J Neuroradiol. 2006;27:2005–11.
10. Ropele S, Langkammer C, Enzinger C, Fuchs S, Fazekas F. Relaxation time mapping in multiple sclerosis. Expert Rev Neurother. 2011;11:441–50.
11. MacKay AL, Vavasour IM, Rauscher A, Kolind SH, Mädler B, Moore GR, Traboulsee AL, Li DK, Laule C. MR relaxation in multiple sclerosis. Neuroimaging Clin N Am. 2009;19:1–26.
12. Papadopoulos K, Tozer DJ, Fisniku L, Altmann DR, Davies G, Rashid W, Thompson AJ, Miller DH, Chard DT. TI-relaxation time changes over five years in relapsing-remitting multiple sclerosis. Mult Scler. 2010;16:427–33.

13. Hasan KM, Walimuni IS, Abid H, Datta S, Wolinsky JS, Narayana PA. Human brain atlas-based multimodal MRI analysis of volumetry, diffusimetry, relaxometry and lesion distribution in multiple sclerosis patients and healthy adult controls: implications for understanding the pathogenesis of multiple sclerosis and consolidation of quantitative MRI results in MS. J Neurol Sci. 2012;313:99–109.
14. Jurcoane A, Wagner M, Schmidt C, Mayer C, Gracien RM, Hirschmann M, Deichmann R, Volz S, Ziemann U, Hattingen E. Within-lesion differences in quantitative MRI parameters predict contrast enhancement in multiple sclerosis. J Magn Reson Imaging. 2013;38:1454–61.
15. Warntjes JB, Leinhard OD, West J, Lundberg P. Rapid magnetic resonance quantification on the brain: optimization for clinical usage. Magn Reson Med. 2008;60:320–9.
16. Nöth U, Hattingen E, Bähr O, Tichy J, Deichmann R. Improved visibility of brain tumors in synthetic MP-RAGE anatomies with pure T(1) weighting. NMR Biomed. 2015;28:818–30.
17. Preibisch C, Deichmann R. T1 mapping using spoiled FLASH-EPI hybrid sequences and varying flip angles. Magn Reson Med. 2009;62:240–6.
18. Volz S, Nöth U, Rotarska-Jagiela A, Deichmann R. A fast B1-mapping method for the correction and normalization of magnetization transfer ratio maps at 3 T. Neuroimage. 2010;49:3015–26.
19. Freeman AJ, Gowland PA, Mansfield P. Optimization of the ultrafast Look-Locker echo-planar imaging T1 mapping sequence. Magn Reson Imaging. 1998;16:765–72.
20. Hattingen E, Jurcoane A, Daneshvar K, Pilatus U, Mittelbronn M, Steinbach JP, Bähr O. Quantitative T2 mapping of recurrent glioblastoma under bevacizumab improves monitoring for non-enhancing tumor progression and predicts overall survival. Neuro Oncol. 2013;15:1395–404.
21. Lescher S, Jurcoane A, Veit A, Bähr O, Deichmann R, Hattingen E. Quantitative T1 and T2 mapping in recurrent glioblastomas under bevacizumab: earlier detection of tumor progression compared to conventional MRI. Neuroradiology. 2015;57:11–20.
22. Remmele S, Sprinkart AM, Müller A, Träber F, von Lehe M, Gieseke J, Flacke S, Willinek WA, Schild HH, Sénégas J, Keupp J, Mürtz P. Dynamic and simultaneous MR measurement of R1 and R2* changes during respiratory challenges for the assessment of blood and tissue oxygenation. Magn Reson Med. 2013;70:136–46.
23. Matsumoto K, Bernardo M, Subramanian S, Choyke P, Mitchell JB, Krishna MC, Lizak MJ. MR assessment of changes of tumor in response to hyperbaric oxygen treatment. Magn Reson Med. 2006;56:240–6.
24. Ogawa S, Lee TM, Nayak AS, Glynn P. Oxygenation-sensitive contrast in magnetic-resonance image of rodent brain at high magnetic fields. Magn Reson Med. 1990;14:68–78.
25. Müller A, Remmele S, Wenningmann I, Clusmann H, Träber F, Flacke S, König R, Gieseke J, Willinek WA, Schild HH, Mürtz P. Analysing the response in R2* relaxation rate of intracranial tumours to hyperoxic and hypercapnic respiratory challenges: initial results. Eur Radiol. 2011;21:786–98.